Studying N^* and Δ contributions to exclusive pion production in Proton-Proton Collisions using HADES data

Saket Kumar Sahu[1,2,*], *Johan* Messchendorp[2,1] and *James* Ritman[2,1] for the HADES collaboration

[1]Ruhr University Bochum, Universitätsstraße 150, 44801 Bochum, Germany
[2]GSI Helmholtzzentrum fur Schwerionenforschung GmbH, Planckstraße 1, 64291 Darmstadt, Germany

Abstract. Excited nucleon states (N^* and Δ resonances) provide an important probe of the non-perturbative regime of Quantum Chromodynamics (QCD) and the internal structure of baryons. In this work, we study the production mechanisms of these resonances in the reaction $pp \rightarrow NN\pi$. The High Acceptance Di-Electron Spectrometer (HADES) at GSI Darmstadt, a versatile magnetic spectrometer with large angular acceptance, is well suited for such studies. This analysis focuses on the exclusive production of N^* and Δ channels in proton-proton collisions at $\sqrt{s}$ = 3.47 GeV/c^2 and aims to extract their coupling strengths. We present results from the analysis of data collected by the HADES collaboration in February 2022, together with preliminary comparisons to fits obtained using the Jülich-Bonn (JüBo) dynamical coupled-channel model. Finally, we discuss the applicability of the fitting framework, implemented with AmpTools, to other exclusive channels, including reactions involving strangeness.

1 Introduction

The production of excited nucleon states in proton-proton collisions provides an important probe for investigating the dynamics of the strong interaction in the non-perturbative regime of Quantum Chromodynamics (QCD)[1]. Their radiative transitions and decays provide valuable information on their electromagnetic structure. In particular, virtual-photon transitions of excited nucleon states, $N^* \rightarrow N\gamma^*$ and $\Delta \rightarrow N\gamma^*$, offer access to observables that cannot be obtained from real-photon measurements. However, the electromagnetic currents governing these decays remain poorly understood because of the short lifetimes of the resonances ($\sim 10^{-23}$ s) [2] and the scarcity of experimental data on their time-like electromagnetic transitions [3, 4]. Previous HADES studies using proton-proton scattering at T = 1.25 [5], 2.2 GeV [6] and 3.5 GeV [7] followed this strategy and provided valuable high statistics differential data on pion production, for which the available experimental database remains limited. A prerequisite for investigating their electromagnetic structure is therefore a detailed understanding of the production and hadronic decays of the contributing N^* and Δ resonances. Their study also contributes to addressing fundamental questions, such as the relationship between dynamically generated resonances and those predicted by constituent quark models [1].

*e-mail: s.k.sahu@gsi.de

In these proceedings, we investigate the production mechanisms of these resonances in the reaction $pp \rightarrow NN\pi$ which complements existing information from photon and pion induced reactions. The proton-proton data analysed in this work were collected during the FAIR Phase-0 program with the High Acceptance Di-Electron Spectrometer (HADES) at GSI Darmstadt, a versatile magnetic spectrometer with large angular acceptance.

2 Particle Identification in HADES

HADES is a fixed-target magnetic spectrometer comprising six sectors and covering polar angles from 18° to 85°. Charged-particle trajectories and momenta are reconstructed with four planes of Mini Drift Chambers surrounding a superconducting magnet, while the RPC, TOF, and Inner Time-of-Flight (iTOF) detectors provide time-of-flight information. The setup also includes an electromagnetic calorimeter for photon detection and a Forward Detector which extends the acceptance to small polar angles. A detailed description of the HADES setup used during the proton-proton measurement is given in [8]. The present analysis uses 1/30 of the proton-proton data collected at a center-of-mass energy ($\sqrt{s}$) of 3.47 GeV/c^2. Events were preselected by requiring at least two iTOF and RPC/TOF coincidences plus at least one additional hit in the iTOF. Exactly two reconstructed positively charged tracks were also required.

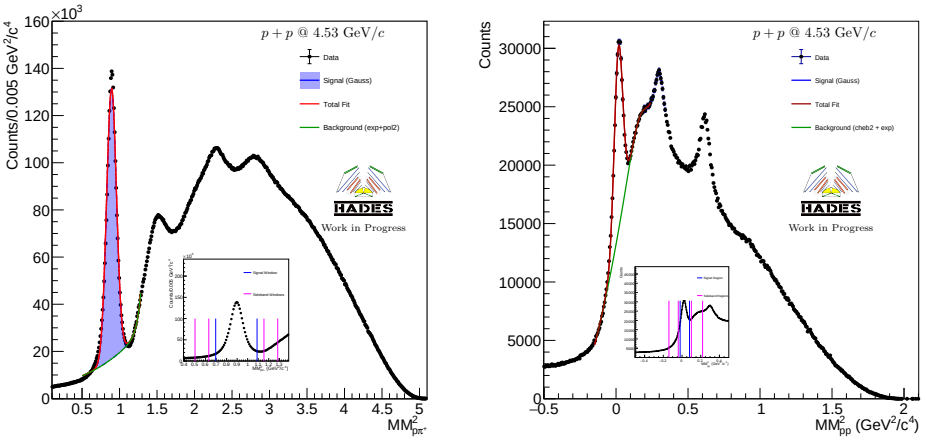

(a) (b)

Figure 1: Squared missing-mass distributions of the detected (a) $p\pi^+$ and (b) pp systems. The signal and sideband regions are indicated in the insets. The indicated peaks in the spectra around the neutron and pion mass squared represent the $pn\pi^+$ and $pp\pi^0$ final states, respectively.

Particle identification was based on the relative time-of-flight, $\Delta T = T_{\text{meas}} - T_{\text{exp}}$. For each track, T_{exp} was calculated from its momentum, path length, and the mass assigned under a proton or pion hypothesis. The hypothesis combination with the minimum χ^2 was selected. The undetected neutron in $pp \rightarrow pn\pi^+$ and π^0 in $pp \rightarrow pp\pi^0$ were reconstructed using the missing-mass technique. Elastic (pp) events were suppressed using their characteristic two-body kinematics, i.e., the coplanarity condition ($\Delta\phi = |\phi_1 - \phi_2| = 180°$) and $\tan\theta_1 \tan\theta_2 =$

$1/\gamma^2_{\mathrm{CM}}$. Events within this kinematic region were rejected, thereby enhancing inelastic $pp\pi^0$ candidates. Background contributions were estimated using sidebands on the left- and right-hand side of the signal regions in the missing-mass spectra, as indicated in the insets of Fig.1. A Lagrange-multiplier-based kinematic fitter (KinFit) [9] was used to map the sideband event kinematics into the corresponding signal regions and to reconstruct the four-momenta of the undetected particles.

3 Dalitz Plots and JüBo Model

Fig.2 shows the Dalitz plots of the $pn\pi^+$ and $pp\pi^0$ final states after sideband subtraction. The data demonstrates that most of the kinematically allowed phasespace is covered and the missing part of the phase space is the acceptance cut for $\theta_p < 15^\circ$ and acceptance cut for $\theta_{\pi^+} < 15^\circ$. The $pn\pi^+$ Dalitz plot (Fig.2a) presented as function of $M^2_{p\pi^+}$ and $M^2_{n\pi^+}$, shows a clear enhancement near $M^2_{p\pi^+} \approx 1.5$ GeV$^2/c^4$, as well as structures around $M^2_{n\pi^+} \approx 2.3$ and 2.8 GeV$^2/c^4$. Similarly, the $pp\pi^0$ Dalitz plot (Fig.2b) shows clear enhancements near $M^2_{p\pi^0} \approx 2.3$ and 2.7 GeV$^2/c^4$. Compared with the $p\pi^+$ distribution, the $p\pi^0$ distribution is suppressed around $M^2_{p\pi^0} \approx 1.5$ GeV$^2/c^4$. The structures observed in the Dalitz plots indicate contributions from several N^* and Δ^* resonances. A quantitative determination of the individual resonance contributions and their interferences require an amplitude analysis of the data. Although the Bonn-Gatchina Partial Wave Analysis (PWA) framework has been applied to $pp \to NN\pi$ reactions at lower energies [10], no corresponding amplitude analysis is currently available for $pp \to NN\pi$ ($2 \to 3$ body) reaction at $\sqrt{s} = 3.47$ GeV/c^2. Therefore an approach based on the Jülich Bonn (JüBo) dynamical coupled-channel model was developed to describe the present data.

The Jülich-Bonn dynamical coupled-channel (JüBo DCC) model is a theoretically well defined approach based on the meson-exchange picture, which respects (2-body) unitarity and analyticity [11]. The meson-baryon interactions have been constrained through a large part of the pion- and photo-production world data. We model the $NN\pi$ final state by treating one of the nucleons as a spectator and the other nucleon as a participant in the $N\pi$ subsystem. The $N\pi$ subsystem is described by the JüBo DCC model, which includes contributions from several N^* and Δ^* resonances. The amplitude for a given partial wave is constructed as

$$\mathcal{A}_{LIJ} = B_L(q)\sqrt{\frac{\rho(s,m_1,m_2)K_f}{K_i}}\mathcal{A}_{J\ddot{u}Bo}(\alpha,\Gamma) \tag{1}$$

where $\mathcal{A}_{J\ddot{u}Bo}(\alpha,\Gamma) = \alpha_j(\epsilon - \epsilon_{thr}) + \sum_k^{Channels}\beta_k\Gamma_k(\epsilon) + \sum_i^{Resonances}\gamma_i\Gamma_i^{(R)}(\epsilon)$, $B_L(q) = q^L$ is the Blatt-Weisskopf barrier factor for a spectator with the orbital angular momentum L, $\rho(s,m_1,m_2)$ is the phase space factor, K_f and K_i are the final and initial state momenta in the center of mass frame, $\Gamma_k(\epsilon)$ and $\Gamma_i^R(\epsilon)$ are the complex amplitudes of non resonant background and resonance contributions respectively. ϵ is the two-body meson-baryon center-of-mass energy. α_j, β_k and γ_i are the fit parameters. The $N\pi$ amplitudes obtained from the JüBo DCC model are provided in tabulated form for orbital angular momenta up to $L = 5$ and two-body center-of-mass energies ranging from 1.07 to 2.5 GeV/c^2. As shown in Eq.1, these amplitudes are multiplied by a Blatt-Weisskopf barrier factor to model the spectator nucleon.

We perform an event-by-event maximum-likelihood fit to the $pn\pi^+$ data using the AmpTools framework [12]. The fit shown in Fig. 3 includes four partial waves, namely P_{33}, P_{31}, S_{11}, and P_{11}, which are added coherently. The sideband events are included in the likelihood with negative weights to account for the background contribution. For comparison with the

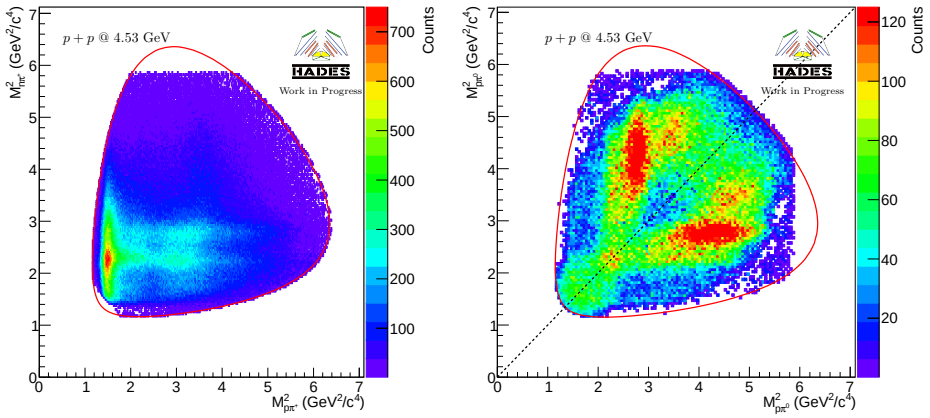

(a) (b)

Figure 2: Sideband subtracted Dalitz plot for the (a) $pn\pi^+$ and (b) $pp\pi^0$ final state. The red outlines show the kinematical limits of the occupied phase space for the $pp \to pn\pi^+$ and $pp \to pp\pi^0$ reactions, respectively.

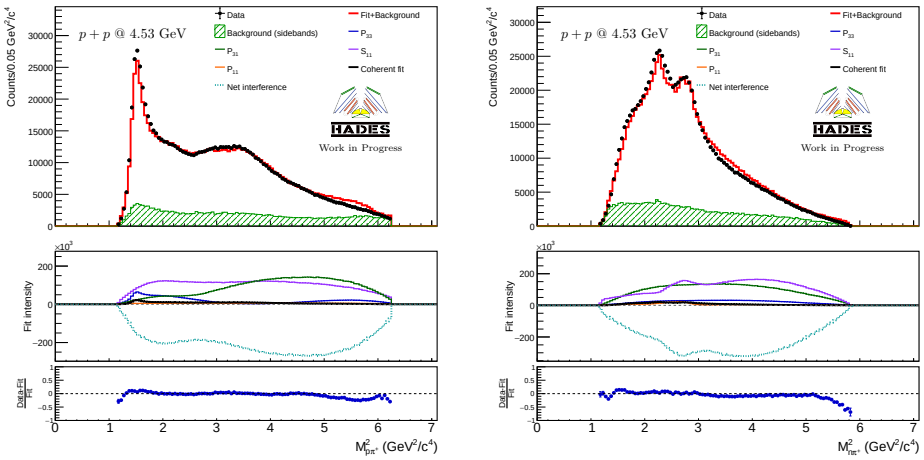

(a) (b)

Figure 3: Projections of the $pn\pi^+$ Dalitz plot onto (a) $M^2_{p\pi^+}$ and (b) $M^2_{n\pi^+}$. The upper panels compare the data with the coherent fit and sideband background. The middle panels show the individual-wave intensities, their incoherent sum, and the net interference. The lower panels show (Data – Fit)/Fit.

unsubtracted data, the estimated sideband background is added incoherently to the coherent signal model fit. Detector acceptance and reconstruction efficiency are accounted for in the fit using reconstructed Monte Carlo events generated according to three-body $pn\pi^+$ phase space. The resulting amplitude provides a reasonable description of the measured distributions.

The P_{33} wave dominates the low-mass region of the $p\pi^+$ invariant mass spectrum Fig. 3a, consistent with the expected dominant contribution of the $\Delta^{++}(1232)$ resonance, while the remaining partial waves contribute predominantly at higher invariant masses. The middle panel of Fig. 3 shows the individual-wave intensities and the net interference contribution. A strong destructive interference between the fitted amplitudes is observed. Consequently, the individual-wave intensities are highly model dependent and should not be interpreted as independent resonance yields. A quantitative extraction of the resonance contributions will require systematic studies using alternative wave sets and fit parametrizations.

4 Conclusion and Outlook

The exclusive three-body channels $pp \to pn\pi^+$ and $pp \to pp\pi^0$ were identified with high statistics. Preliminary fits to the $pp \to pn\pi^+$ channel demonstrate the feasibility of incorporating coupled-channel amplitudes into the description of the three-body final state. This approach represents a first step towards developing a comprehensive partial-wave-analysis framework for $NN \to NN\pi$ reactions.

Future studies will include a detailed evaluation of the statistical and systematic uncertainties of the fit results, as well as the incorporation of the angular dependence of the partial waves into the amplitude calculation. A combined analysis of the $pp \to pn\pi^+$ and $pp \to pp\pi^0$ channels is planned to provide stronger constraints on the contributing N^* and Δ^* resonances. The framework developed in this work may be extended to other exclusive final states. Because the JüBo model also includes the coupling to the $K\Lambda$ and $K\Sigma$ channels, the same partial wave set applies directly to strangeness production reactions such as $pp \to pK^+\Lambda$ and $pp \to pK^+\Sigma^0$. Ultimately, these studies aim to establish a consistent description of baryon resonance production in proton-proton collisions, providing an essential hadronic reference for future investigations of their electromagnetic transitions and for the interpretation of heavy-ion collision data.

5 Acknowledgments

We thank the Jülich Bonn group, particularly Deborah Rönchen, for providing the tabulated JüBo DCC amplitudes and for many stimulating discussions. We also thank Christoph Hanhart for his valuable suggestions and guidance throughout the development of this framework.

References

[1] V. Burkert, G. Eichmann, E. Klempt, The impact of γN and $\gamma^* N$ interactions on our understanding of nucleon excitations. Progress in Particle and Nuclear Physics **146**,104214 (2026). https://doi.org/10.1016/j.ppnp.2025.104214

[2] S. Schumann et al., Radiative π^0 photoproduction on protons in the Δ^+ (1232). The European Physical Journal A **43**, 269-282 (2010). https://doi.org/10.1140/epja/i2010-10925-y

[3] HADES Collaboration., J. Adamczewski-Musch et al., $\Delta(1232)$ Dalitz decay in proton-proton collisions at $T = 1.25$ GeV measured with HADES at GSI. Phys. Rev. C **95**, 065205 (2017). https://link.aps.org/doi/10.1103/PhysRevC.95.065205

[4] HADES Collaboration., R. Abou Yassine et al., First measurement of massive virtual photon emission from N* baryon resonances. Physics Letters B **875**, 140338 (2026). https://doi.org/10.1016/j.physletb.2026.140338

[5] Witold Przygoda et al., Investigating hadronic resonances in pp interactions with HADES. EPJ Web of Conferences **97**, 00024 (2015). https://doi.org/10.1051/epjconf/20159700024

[6] HADES Collaboration., G. Agakishiev et al., Study of exclusive one-pion and one-eta production using hadron and dielectron channels in pp reactions at kinetic beam energies of 1.25 GeV and 2.2 GeV with HADES. The European Physical Journal A **48**, 74 (2012). https://doi.org/10.1140/epja/i2012-12074-9

[7] HADES Collaboration., G. Agakishiev et al., Baryon resonance production and dielectron decays in proton-proton collisions at 3.5 GeV. The European Physical Journal A **50**, 82 (2014). http://dx.doi.org/10.1140/epja/i2014-14082-1

[8] HADES Collaboration., R. Abou Yassine et al., Measurement of Differential Cross Sections and Integrated Luminosity using Proton-Proton Elastic Scattering with HADES at T = 4.53 GeV and T = 1.60 GeV. arXiv:2609.02989, **hep-ex** (2026). https://arxiv.org/abs/2609.02989

[9] E. Waleed et al., KinFit: A Kinematic Fitting Package for Hadron Physics Experiments. Computing and Software for Big Science **8**, 3 (2024). https://doi.org/10.1007/s41781-023-00112-x

[10] HADES Collaboration., Agakishiev, G., Balanda, A. et al., Analysis of pion production data measured by HADES in proton-proton collisions at 1.25 GeV. The European Physical Journal A **51**, 137 (2015). https://doi.org/10.1140/epja/i2015-15137-5

[11] D. Rönchen et al., Coupled-channel dynamics in the reactions $\pi N \to \pi N, \eta N, K\Lambda, K\Sigma$. The European Physical Journal A **49**, 44 (2013). https://doi.org/10.1140/epja/i2013-13044-5

[12] M. Shepherd et al., mashephe/AmpTools: Version 0.15.3, Zenodo **v0.15.3** (2024). https://doi.org/10.5281/zenodo.10961168